



Symmetry-adapted formulation of the hybrid treatment resulting from the G-particle-hole Hypervirial equation and equations of motion methods: a procedure for modeling solids

Juan J. Torres-Vega¹ · Gustavo E. Massaccesi² · Elías Ríos³ · Alberto Camjayi^{4,5} · Alicia Torre⁶ · Luis Lain⁶ · Ofelia B. Oña³ · William Tiznado⁷ · Diego R. Alcoba^{4,5}

Received: 19 September 2020 / Accepted: 18 December 2020 / Published online: 2 January 2021
© The Author(s), under exclusive licence to Springer Nature Switzerland AG part of Springer Nature 2021

Abstract

Highly accurate electron affinities and ionization potentials of chemical systems were described by means of the procedure called GHV-EOM (Valdemoro et al, in Int J Quantum Chem 112:2965, 2012), which combines the G-particle-hole hypervirial (GHV) equation method (Alcoba et al, in Int J Quantum Chem 109:3178, 2009) and that of the equations-of-motion (EOM), by Simons and Smith (Simons and Smith, in J Chem Phys 58:4899, 1973). The present work improves that hybrid method by introducing the point group symmetry within its framework, providing a higher computational efficiency. We report results which show the achievements attained by using the symmetry-adapted methodology. The new formulation turns out to be particularly suitable for characterizing solid models, as cyclic one-dimensional chains.

Keywords Reduced density matrix · Hypervirial · Equations of motion · Point group symmetry · Solid model

1 Introduction

According to quantum mechanics principles, all the information required to describe N -electron systems is contained in their corresponding N -electron wave functions. However, as is well known, in most situations the management of these devices turn out to be too cumbersome. Consequently, alternative tools have been searched to describe that kind of systems. A successful procedure, proposed long time ago [1–5], is the use of reduced density matrices. The elements of these matrices can be determined by

✉ Diego R. Alcoba
dalcoba@df.uba.ar

Extended author information available on the last page of the article

means of variational and non-variational methods [6–12], allowing one to get rid of the N -electron wave functions. Moreover, each one of the terms involved in the formulation of an N -electron Hamiltonian can be classified into two categories (of one- and two-body type) according to the nature of the physical interactions they represent. Hence, the determination of N -electron properties requires the implementation of methods trying to achieve suitable approximations to evaluate the elements of the second-order reduced density matrix (2-RDM).

Among the non-variational methods providing the calculation of the elements of the 2-RDMs, a considerable interest has been devoted to the iterative solution of the G-particle-hole hypervirial equation (GHV) [13], which is closely related to the anti-Hermitian contracted Schrödinger equation [14] and arises from a contraction of a particular case of the quantum Liouville equation [15]. The results obtained from the GHV method have turned out to be very close to those provided by the full configuration interaction (FCI) procedure for ground states of molecular systems, as at equilibrium geometries as at distorted ones [13, 16–18]. In a subsequent step, these results induced some of us to combine the GHV method with the equations of motion (EOM) treatment reported by Simons and Smith [19] for the calculation of electron affinities (EA) and ionization potentials (IP). These energies were directly evaluated from the corresponding ground state 2-RDMs or, in an equivalent manner, from the G-particle-hole matrices obtained by solving the GHV equation. The results show that this combined GHV-EOM method yields very accurate EA and IP values [20]. The aim of this work is to further improve the efficiency of the combined GHV-EOM method by using point group symmetry. Following recent treatments carried out within the framework of the GHV method [21, 22], a symmetry-related analysis of the matrices and matrix operations involved in the EOM method is performed. This analysis allows one to formulate a symmetry-adapted version of the combined GHV-EOM algorithm for Abelian groups, which leads to significant computational savings in both floating-point operations and memory storage.

We have organized this work as follows. In the second section we report the definitions, notations, and a general theoretical background of the GHV and EOM methods. In the third section we describe the symmetry-adapted formulation of the GHV-EOM treatment. In section four we analyze the results obtained for a set of small-to-medium-sized cyclic one-dimensional hydrogen chains showing the performance and efficiency of this new formulation. This kind of systems has been widely used as prototype model to describe solids in quantum chemistry, condensed matter, and solid state physics [23–27]; they present some interesting features that are essential for testing the suitability of theoretical methods to describe real systems, as the presence of strong correlation of diverse nature depending on the H-H distance. Finally, in the last section, we report the conclusions of this work.

2 Theoretical background

2.1 Notation and definitions

Let us consider an N -electron system whose Hamiltonian, \hat{H} , in the second quantization formalism can be written as [28]

$$\hat{H} = \sum_{p,r} \epsilon_r^p a_p^\dagger a_r + \frac{1}{2} \sum_{p,q,r,s} V_{rs}^{pq} a_p^\dagger a_q^\dagger a_s a_r \quad (1)$$

where a_p^\dagger and a_r are the usual creation and annihilation operators, respectively, and the indices $\{p, q, r, s, \dots\}$ stand for the $2K$ orthonormal spin-orbitals of a finite basis set. ϵ_r^p and $V_{rs}^{pq} = \langle pq|rs \rangle$ (in the $\langle 12|12 \rangle$ convention) are the one- and two-electron integrals, respectively.

One can define a two-body matrix which collects the one- and two-electron integrals

$$H_{rs}^{pq} = \frac{\epsilon_r^p \delta_s^q + \epsilon_s^q \delta_r^p}{N-1} + V_{rs}^{pq} \quad (2)$$

in which the symbols δ mean the Kronecker deltas. Equation (2) allows one to express the \hat{H} operator in a more compact manner

$$\hat{H} = \frac{1}{2} \sum_{pq,rs} H_{rs}^{pq} a_p^\dagger a_q^\dagger a_s a_r \quad (3)$$

According to this formalism, the elements of the first- and second-order reduced density matrices (1- and 2-RDM) [28] and those of the second-order G-particle-hole correlation matrix [6] corresponding to an N -electron wave function Φ may, respectively, be expressed as

$${}^1D_v^t = \langle \Phi | a_t^\dagger a_v | \Phi \rangle, \quad (4)$$

$${}^2D_{kl}^{ij} = \frac{1}{2!} \langle \Phi | a_i^\dagger a_j^\dagger a_l a_k | \Phi \rangle \quad (5)$$

and

$${}^2G_{ij}^{im} = \langle \Phi | {}^2\hat{G}_{ij}^{im} | \Phi \rangle = \sum_{\Phi' \neq \Phi} \langle \Phi | a_i^\dagger a_m | \Phi' \rangle \langle \Phi' | a_j^\dagger a_l | \Phi \rangle. \quad (6)$$

The elements of these three matrices, which are related by Mihailovic and Rosina equation [29]

$$2! {}^2D_{ml}^{ij} = {}^1D_m^i {}^1D_l^j - {}^1D_l^i \delta_m^j + {}^2G_{ij}^{im} \quad (7)$$

are the basic tools of the GHV and EOM methodologies, described in the two next subsections.

2.2 The G-particle-hole hypervirial equation method

By applying a contracting mapping involving a G-particle-hole operator ${}^2\hat{G}$ to the matrix representation of the hypervirial relation of the N -electron density operator (a particular case of the quantum Liouville equation), one obtains the GHV equation [13, 15], whose compact form is

$$\left\langle \Phi \left| \left[\hat{H}, {}^2\hat{G}_{lj}^{im} \right] \right| \Phi \right\rangle = 0 \quad (\forall i, j, l, m) \quad (8)$$

and its explicit development leads to [13]

$$\begin{aligned} & \sum_{p,q,r,s} H_{pq}^{rs} {}^{(3;2,1)}C_{rsl}^{pqj} {}^1D_m^i - \sum_{p,q,r,s} H_{rs}^{pq} {}^{(3;2,1)}C_{pqi}^{rsm} {}^1D_j^l \\ & + 2 \sum_{p,r,s} H_{pm}^{rs} {}^{(3;2,1)}C_{rsl}^{ipj} + 2 \sum_{p,q,r} H_{jr}^{pq} {}^{(3;2,1)}C_{pqi}^{lrm} \\ & + 2 \sum_{p,q,r} H_{pq}^{ir} {}^{(3;2,1)}C_{mrl}^{pqj} + 2 \sum_{q,r,s} H_{rs}^{ql} {}^{(3;2,1)}C_{jq_i}^{rsm} = 0 \end{aligned} \quad (9)$$

where

$${}^{(3;2,1)}C_{pqt}^{ijm} = \sum_{\Phi' \neq \Phi} \langle \Phi | a_i^\dagger a_j^\dagger a_q a_p | \Phi' \rangle \langle \Phi' | a_m^\dagger a_t | \Phi \rangle \quad (10)$$

are the elements of a third-order correlation matrix [30].

The GHV equation depends on the elements of the 1- and 2-RDMs as well as those of the third-order correlation matrix. However, the elements of this last matrix can be approximated in terms of the lower-order ones [10, 12, 17, 31–33]. In this work we have used a modified version of the Nakatsuji-Yasuda's approximation algorithm [10, 17], which leads to a solution of the GHV equation by means of an iterative procedure. It consists in solving a set of differential equations minimizing the second-order error matrix resulting from the deviation from exact fulfilment of the equation. This procedure yields an approximated G-particle-hole matrix corresponding to the eigenstate being studied [16].

2.3 The equations of motion method

The EOM method [34, 35] was applied by Simons and Smith [19] to describe properties of the electron-addition and electron-removal subspaces of an N -electron state. This method allows one to compute electron affinities and ionization potentials of an N -electron system from the sole knowledge of its ground-state 2-RDM, or from the corresponding G-particle-hole matrix. The procedure is based on two relations connecting an N -electron neutral reference state $\Phi(N)$ of the Hamiltonian with the corresponding $(N + 1)$ -electron anion and $(N - 1)$ -electron cation states, $\Psi(N + 1)$ and $\Psi(N - 1)$ respectively, by means of an operator \hat{S} :

$$\hat{H} \hat{S} |\Phi(N)\rangle = E_{\Psi} |\Psi(N-1)\rangle \quad (11a)$$

$$\hat{H} \hat{S}^{\dagger} |\Phi(N)\rangle = E_{\Psi} |\Psi(N+1)\rangle, \quad (11b)$$

which requires to solve the equations

$$\langle \Phi | \hat{S} [\hat{H}, \hat{S}'^{\dagger}] | \Phi \rangle = \Delta E^{+} \langle \Phi | \hat{S} \hat{S}'^{\dagger} | \Phi \rangle \quad (12a)$$

$$\langle \Phi | [\hat{H}, \hat{S}'^{\dagger}] \hat{S} | \Phi \rangle = \Delta E^{-} \langle \Phi | \hat{S}'^{\dagger} \hat{S} | \Phi \rangle \quad (12b)$$

where ΔE^{+} and ΔE^{-} provide the electron affinity and ionization potential energies, respectively. By expanding the \hat{S} operator in the basis set of \hat{S}' operators, both equations become linear and can be combined as follows [36, 37]:

$$\langle \Phi | [\hat{S}, [\hat{H}, \hat{S}'^{\dagger}]_{+} | \Phi \rangle = \Delta E \langle \Phi | \hat{S} \hat{S}'^{\dagger} + \hat{S}'^{\dagger} \hat{S} | \Phi \rangle, \quad (13)$$

where ΔE allows to compute either electron affinity or ionization potential energies. The latter equation permits to simultaneously evaluate the energy differences of Eqs. (12a) and (12b) and to reduce the computational cost, because the anticommutation implies a cancellation of the higher order matrices.

Different approximations of the \hat{S} operator have been proposed to solve these equations [20, 37–39]. In this work, for simplicity, we will formulate the \hat{S} operator as

$$\hat{S} = \sum_t c_t a_t \quad (14)$$

where the c symbols are real coefficients. By replacing this definition into Eqs. (12b), one obtains the following system of equations for the electron affinities and ionization potentials $\Delta E^{(\pm)}$ and the expansion vectors $c^{(\pm)}$

$$\mathcal{H}^{(\pm)} c^{(\pm)} = \Delta E^{(\pm)} \mathcal{M}^{(\pm)} c^{(\pm)} \quad (15)$$

where $\mathcal{M}^{(\pm)}$ and $\mathcal{H}^{(\pm)}$ are functionals of the first-order and first- and second-order reduced density matrices corresponding to the reference eigenstate, respectively, which have the following form

$$\mathcal{M}_q^{p(+)} = \delta_q^p - {}^1D_q^p \quad \mathcal{M}_q^{p(-)} = {}^1D_q^p \quad (16)$$

and

$$\mathcal{H}_q^{p(+)} = \epsilon_q^p - \sum_i \epsilon_q^i {}^1D_i^p + \sum_{ij} \tilde{V}_{qj}^{pi} {}^1D_i^j + \sum_{ij,l} \tilde{V}_{ql}^{ij} {}^2D_{ij}^{lp} \quad (17)$$

$$\mathcal{H}_q^{p(-)} = \sum_i \epsilon_q^i {}^1D_i^p - \sum_{ij,l} \tilde{V}_{ql}^{ij} {}^2D_{ij}^{lp} \quad (18)$$

with

$$\tilde{V}_{ps}^{ir} \equiv V_{ps}^{ir} - V_{sp}^{ir} \quad (19)$$

When combined, these two systems of equations are reduced to

$$\mathcal{H} c = \Delta E c \quad (20)$$

where the matrix \mathcal{H} has the following form

$$\mathcal{H}_q^p = \epsilon_q^p + \sum_{i,j} \tilde{V}_{qj}^{pi} D_i^j \quad (21)$$

Equations (15) and (20) constitute generalized eigenvalue systems depending on the 2-RDM (or on the G-particle-hole matrix) and on the 1-RDM, respectively, which may be obtained solving the GHV equation. That is the main reason why the RDM-oriented methods and the EOM one have been combined [20, 38–40]. In the next section we describe the algorithm, based on the point group symmetry, which greatly improves the computational efficiency of the combined GHV-EOM method.

3 Symmetry-adaptation of the GHV-EOM method

3.1 The covariant equations

The operations of the symmetry point group \mathcal{F} , corresponding to an N -electron system, maintain unchanged the one- and two-electron integral matrices ϵ and V and therefore, these matrices are invariant (1,1)- and (2,2)-tensors, respectively, for that group [41]. Similarly, if the N -electron wave function Φ belongs to a one-dimensional representation of the \mathcal{F} group, its corresponding 1- and 2-RDM and G-particle-hole matrix are invariant and, consequently, the 1-RDM is (1,1)-tensor and the 2-RDM and the G-particle-hole matrix are (2,2)-tensors for that symmetry point group [41]. Moreover, when the spin-orbitals are symmetry adapted and ordered according to their irreducible representations, these one- and two-electron matrices are sparse and, if \mathcal{F} is Abelian, they turn out to be block diagonal. In all these matrices the symmetry forbidden coefficients present a structure which is easier to analyze if the \mathcal{F} group possesses an Abelian D_{2h} subgroup. Consequently, hereafter only this type of groups will be considered. When the N -electron system has not an Abelian symmetry group, an Abelian subgroup will be considered.

The sparsity of the 1- and 2-RDMs has been studied within the framework of the GHV methodology, performing an analysis of the matrix operations involved in Eq. (9). This analysis provides a symmetry-adapted formulation of the GHV algorithm, generating significant computational savings in floating-point operations as well as in memory storage [21]. In the case of the EOM equations, the analysis of Eqs. (15) and (20) requires to calculate three different types of terms,

$$\sum_i \epsilon_q^i D_i^p \equiv {}^1X_q^p \quad (22)$$

$$\sum_{i,j} \tilde{V}_{qj}^{pi} {}^1D_i^j \equiv {}^1Y_q^p \quad (23)$$

and

$$\sum_{i,j,l} \tilde{V}_{ql}^{ij} {}^2D_{ij}^{lp} \equiv {}^1Z_q^p \quad (24)$$

A survey of the mathematical operations required for the calculation of these terms shows that the corresponding auxiliary and final matrices are formulated by covariant equations. Those matrices can be expressed by means of tensorial operations as follows:

$${}^1X = \left((\epsilon \otimes {}^1D)_{(1,2) \rightarrow (2,1)}^{(1,2) \rightarrow (2,1)} \right)_{\text{con}} \quad (25)$$

$${}^1Y = \left(\left((\tilde{V} \otimes {}^2D)_{(1,2,3) \rightarrow (1,3,2)}^{(1,2,3) \rightarrow (1,2,3)} \right)_{\text{con}} \right)_{\text{con}} \quad (26)$$

$${}^1Z = \left(\left(\left((\tilde{V} \otimes {}^2D)_{(1,2,3,4) \rightarrow (1,2,3,4)}^{(1,2,3,4) \rightarrow (4,3,1,2)} \right)_{\text{con}} \right)_{\text{con}} \right)_{\text{con}} \quad (27)$$

where

$$(\mathbf{V} \otimes \mathbf{W})_{m_1 \dots m_{v+w}}^{i_1 \dots i_{v+w}} = V_{m_1 \dots m_v}^{i_1 \dots i_v} \times W_{m_{v+1} \dots m_{v+w}}^{i_{v+1} \dots i_{v+w}} \quad (28)$$

$$\left(\mathbf{V} \begin{matrix} (1, \dots, v) \rightarrow (\tau(1), \dots, \tau(v)) \\ (1, \dots, v) \rightarrow (\sigma(1), \dots, \sigma(v)) \end{matrix} \right)_{m_1 \dots m_v}^{i_1 \dots i_v} = V_{m_{\sigma(1)} \dots m_{\sigma(v)}}^{i_{\tau(1)} \dots i_{\tau(v)}} \quad (29)$$

$$(\mathbf{V}_{\text{con}})_{m_1 \dots m_{v-1}}^{i_1 \dots i_{v-1}} = \sum_x V_{m_1 \dots m_{v-1}, x}^{i_1 \dots i_{v-1}, x} \quad (30)$$

The covariance of these equations entails that all matrices involved in EOM method are invariant tensors for the \mathcal{F} group, which maintains the symmetry properties of the input density and electron integral matrices. These tensors possess a block structure, which provides an efficient evaluation of the EOM operations for each one of the operations resulting from Eqs. (15) and (20). For instance, the matrix 1X defined in Eq. (22) is a (1,1)-tensor for the \mathcal{F} group whose non-vanishing blocks are associated with each irreducible representation π of \mathcal{F} . Consequently, one can avoid the evaluation of the symmetry forbidden elements and calculate the remaining ones according to

$${}^1X_q^p = \sum_{i \in \pi} \epsilon_q^i {}^1D_i^p \quad (\forall p, q \in \pi) \quad (31)$$

In a similar way, the auxiliary matrices 1Y and 1Z defined in Eqs. (23) and (24) can be evaluated as

$${}^1Y_q^p = \sum_{\tilde{\pi}} \sum_{i,j \in \tilde{\pi}} \tilde{V}_{qj}^{pi} {}^1D_i^j \quad (\forall p, q \in \pi) \quad (32)$$

and

$${}^1Z_q^p = \sum_{\pi_i, \pi_j, \pi_l} \sum_{i \in \pi_i, j \in \pi_j, l \in \pi_l} \tilde{V}_{ql}^{ij} {}^2D_{ij}^{lp} \quad (\forall p, q \in \pi) \quad (33)$$

$$\pi_i \otimes \pi_j = \pi \otimes \pi_l$$

The remaining matrix operations required for the solution of the generalized eigenvalue equations in the EOM method can be treated in an identical manner. Consequently, the block structure of the ordinary density and electron integral matrices presented in the EOM equations yields a more efficient procedure for the EOM numerical determinations, reducing the computational costs. In the next subsection, we discuss and analyze the advantages of a symmetry-adapted formulation of the GHV-EOM (sa-GHV-EOM) method resulting from combining the symmetry-adapted formulations of the GHV (sa-GHV) and EOM (sa-EOM) algorithms.

3.2 Efficiency of the sa-GHV-EOM method

If the \mathcal{F} group possesses f irreducible representations, and assuming that the distribution of molecular spin-orbitals according to the irreducible representations is strictly regular, a straightforward calculation shows that the (1, 1)-tensors have f blocks of size $(K/f) \times (K/f)$, having K^2/f^2 non-vanishing coefficients, and the (2, 2)-tensors have f blocks of size $(K^2/f) \times (K^2/f)$ with K^4/f^2 non-vanishing coefficients. The tensor multiplication operations in Eqs. (31), (32), and (33) have a time proportional to $f \times (K/f)^2 \times (K/f) = K^3/f^2$, $f \times (K/f)^2 \times f \times (K/f)^2 = K^4/f^2$, and $f \times (K/f)^2 \times f^2 \times (K/f)^2 \times (K/f) = K^5/f^2$, respectively, and the operations involved in calculation and solution of the generalized eigenvalue Eqs. (15) and (20) require a time proportional to $f \times (K/f)^3 = K^3/f^2$. Similarly as it occurs in the GHV method [21], these estimations indicate that the computational costs of the EOM method are reduced by a factor of f in storage and f^2 in floating-point operations. Obviously, these reductions are only achieved when the symmetry blocking of the orbitals is optimum.

3.3 Application of the sa-GHV-EOM method to describe small-to-medium-sized cyclic one-dimensional atomic chains

Let us consider a simple ring molecule composed of n identical atoms. This system possesses several symmetry elements, but we will focus our attention on a rotation axis, C_n , passing through the center of the ring and perpendicular to the plane of the molecule. Any $C_n^m = m(2\pi/n)$ rotation, being m an integer, maps the molecule onto itself. An usual basis set for treating the problem is the set of atomic orbitals $\{\phi_l^w(\mathbf{r})\}_{l=0, \dots, (n-1); w=a, b, c, \dots}$, where the index l identifies the atom and w identifies the atomic orbital $1s, 2s, 2p_x, 2p_y, 2p_z, \dots$ centered on that atom (with the implicit

convention that $\phi_n^w(\mathbf{r}) = \phi_{l+n}^w(\mathbf{r})$. In general, these orbitals are not symmetry adapted. Consequently, we need to construct a new basis set $\{\chi_j^w(\mathbf{r})\}_{j=0,\dots,(n-1); w=a,b,c,\dots}$, so that its functions turn out to be eigenfunctions of the \hat{C}_n^m rotation operators. These symmetry-adapted functions can be expressed by means of a linear combination of atomic orbitals, and their expansion coefficients c_{jl} can be explicitly calculated or determined using group theory arguments [42]. They are given by $c_{jl} = e^{ik_j l}$, where i stands for the imaginary unit and k_j is

$$k_j = \pm \frac{2\pi}{n}j, \text{ with } j = 0, \dots, \begin{cases} \frac{n-1}{2} & \text{for } n \text{ odd} \\ \frac{n}{2} & \text{for } n \text{ even} \end{cases} \quad (34)$$

It is also possible to consider other values for k_j , although they only differ from those given above by a multiple of 2π and, consequently, they are equivalent.

Let us consider only a s -orbital on each atom. The symmetry-adapted orbitals are then

$$\chi_j^s(\mathbf{r}) = \frac{1}{\sqrt{n}} \sum_{l=0}^{n-1} e^{i\frac{2\pi j}{n}l} \phi_l^s(\mathbf{r}) \quad (35)$$

and the action of the \hat{C}_n^1 operator over the $\chi_j^s(\mathbf{r})$ function is:

$$\hat{C}_n^1 \chi_j^s(\mathbf{r}) = \frac{1}{\sqrt{n}} \sum_{l=0}^{n-1} e^{i\frac{2\pi j}{n}l} \hat{C}_n^1 \phi_l^s(\mathbf{r}), \quad (36)$$

and, since $\hat{C}_n^1 \phi_l^s(\mathbf{r}) = \phi_{l+1}^s(\mathbf{r})$ and $\phi_n^s(\mathbf{r}) = \phi_0^s(\mathbf{r})$ in a closed ring, a simple shift in the dummy summation index gives:

$$\begin{aligned} \hat{C}_n^1 \chi_j^s(\mathbf{r}) &= \frac{1}{\sqrt{n}} \sum_{l=0}^{n-1} e^{i\frac{2\pi j}{n}l} \phi_{l+1}^s(\mathbf{r}) \\ &= \frac{e^{-i\frac{2\pi j}{n}}}{\sqrt{n}} \sum_{l=1}^n e^{i\frac{2\pi j}{n}l} \phi_l^s(\mathbf{r}) = e^{-i\frac{2\pi j}{n}} \chi_j^s(\mathbf{r}). \end{aligned} \quad (37)$$

Obviously the s -orbitals have spherical symmetry, what simplifies the construction of $\chi_j^s(\mathbf{r})$ functions. For p -orbitals it is necessary to apply a local rotation on each atom to guarantee that the action of \hat{C}_n^1 is to map the orbital to an equivalent one on the nearby atom, since $\hat{C}_n^1 \phi_l^{p_z}(\mathbf{r}) = \phi_{l+1}^{p_z}(\mathbf{r})$ but $\hat{C}_n^1 \phi_{l+1}^{p_{xy}}(\mathbf{r}) \neq \phi_{l+1}^{p_{xy}}(\mathbf{r})$, with z perpendicular and x, y on the plane of the ring. New p -orbitals are then defined as:

$$\begin{pmatrix} \phi_l^{p_r} \\ \phi_l^{p_t} \end{pmatrix} = \begin{pmatrix} \cos(2\pi l/N) & \sin(2\pi l/n) \\ -\sin(2\pi l/N) & \cos(2\pi l/n) \end{pmatrix} \begin{pmatrix} \phi_l^{p_x} \\ \phi_l^{p_y} \end{pmatrix}, \quad (38)$$

with the property $\hat{C}_n^1 \phi_{l+1}^{p_{r,t}}(\mathbf{r}) = \phi_{l+1}^{p_{r,t}}(\mathbf{r})$. Proceeding as before, it is now easy to show that $\hat{C}_n^1 \chi_j^{p_{r,t,z}}(\mathbf{r}) = e^{-i\frac{2\pi j}{n}} \chi_j^{p_{r,t,z}}(\mathbf{r})$. This procedure can be repeated on all the orbitals in the basis set until we end up with a fully symmetry-adapted basis.

3.4 Infinite linear chain

For the molecular ring composed of n atoms, we select a set of orbitals belonging to a well defined irreducible representation. The relation $\hat{C}_n^1 \chi_j(r) = e^{-i\frac{2\pi j}{n}} \chi_j(r)$ can be rewritten as $\hat{C}_n^1 \chi_j(r) = e^{-ik_j} \chi_j(r)$, if we define $k_j = \frac{2\pi j}{n}$. This is equivalent to the main property of the Bloch states in a crystal and k_j is associated with the crystal momentum; in particular, $[\hat{C}_n^1]^n$ is the identity operator. This is analogous to the effect of a translation in n lattice constants, hereafter called a , when we consider a fragment of n atoms in a linear chain using the “Born-von Karman” [43] method. Therefore, the molecular ring may be considered a finite approximation to an infinite linear chain. The energies levels ε_j of a ring molecule can be labeled by the k_j values of their irreducible representation, interpreted now as the crystalline moment.

For $n \rightarrow \infty$, the discrete set of energies as a function of $k_j = \frac{2\pi j}{n}$ becomes infinite and the values ε_j are grouped in a set of smooth functions $\varepsilon(k)$ defined for any real k . These functions are 2π periodic and are usually restricted to the first Brillouin zone [42], where $-\pi < ka \leq \pi$ by convention. Note that k is now rescaled by the lattice constant a . The functions $\varepsilon(k)$ are the difference between the singly ionized and neutral systems, that are the so-called energy bands of the crystal.

3.5 Finite size effects

In order to properly describe an infinite chain model by means of a ring molecule, we need to know the finite-size effects. According to this purpose, in this subsection we present the description of a series of systems possessing a broad range of sizes, which are studied at restricted Hartree-Fock (HF) level. The 2-RDMs resulting from that method are introduced into the EOMs in order to obtain the IPs and EAs, allowing to characterize these model bands, although the conclusions are independent of the method used. We show results of H_n rings using the 6-31G** basis set (a set of two s -type and three p -type atomic orbitals assigned to each hydrogen atom), at $R = 1, 1.5$, and 2.5 \AA interatomic distance between two neighbor atoms; the H_{50} has been calculated with the 6-31G basis set. On the left side of Fig. 1 we plot, for several system sizes n , the 1S band obtained. Two effects must be highlighted: the number of energies $\varepsilon(k)$ defining the band increases with n and the shape (dispersion) of the band seems to converge for bigger system sizes. This fact can simply be explained in terms of the number of degrees of freedom of the system; the larger the molecular ring, the higher the number of eigenvalues in the spectrum. Another effect can be pointed out; in small molecules, atoms facing each other across the center of the molecule may have overlapping atomic orbitals and the interaction between them may be important. In an infinite linear chain it would be equivalent to a long range interaction among distant atoms. As the number of atoms in the ring molecule increases so does its radius and, consequently, only interactions between near neighbor atoms become important. Once this limit is reached, one would expect the dispersion of the bands to remain unchanged for $n \rightarrow \infty$. As an illustration of this situation, we plot on the right side of Fig. 1 a simple, nearest neighbor only,

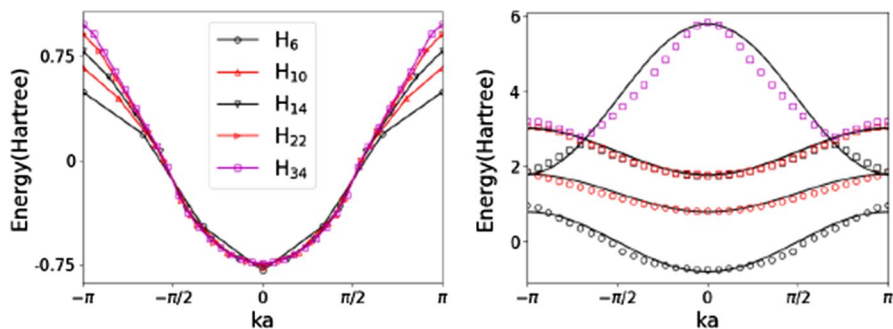


Fig. 1 Finite size effects on H_n ring molecule bands. Left: 1S band of H_n ring molecule for several ring sizes $n = 6, 10, 14, 22,$ and 34 . Right: Simple, nearest neighbor only, tight-binding model fitting for the 1S, 2S, and 2P bands of the H_{34} system. Results correspond to the HF approximation at 1 \AA between two neighbor atoms, using the 6-31G** basis set

tight-binding fit to the 1S, 2S, and 2P bands of the H_{34} system resulting from the HF-EOM approach. It shows the relative importance of short range interactions, even when the fit is not perfect since the HF approximation involves interactions and maybe electronic hopping between atomic orbitals on atoms further than nearest neighbors.

We have considered changes in the size of the molecular ring by modifying the number of atoms constituting that ring. However, it is also possible to fix the number of atoms and adjust the interatomic distance between them (lattice constant). This possibility introduces a different kind of phenomenology from the above discussed one. If we force atoms to be closer to each other, the overlap between orbitals will become important and the delocalization of the electrons would be favored. On the opposite limit, the electrons will be forced to localize and the atomic limit would be reached. The change of site separation works as a parameter that adjusts the relative importance of potential to kinetic energy of electrons. Looking for a suitable physical description, it would be desirable to find the equilibrium separation distance by minimizing the total molecular energy. For large systems, the equilibrium separation distance R_{eq}^n is almost independent on the number n of atoms on the ring. Moreover, as n increases R_{eq}^n quickly converges to a length that equals the bulk lattice constant. Furthermore, a simple test to any implementation is the proper description of the atomic limit. As the atomic separation is increased, the bands should collapse to a set of dispersion-less constants equal to the atomic energies; this effect is observed in Fig. 2.

4 Results and discussion

The sa-GHV-EOM method allows one to obtain IPs and EAs at correlated level with an unexpensive computational cost. Its application to describe crystal models provides the assessment of the incorporation of the electronic correlation in the bands. As previously mentioned for the HF case, here we introduce in our algorithm the

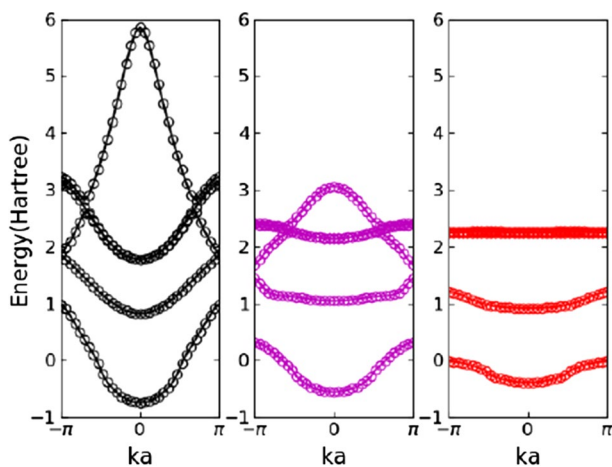


Fig. 2 1S, 2S, and 2P bands of the H_{34} molecular ring with two neighbor atom separation (lattice constant), from left to right, of: 1, 1.5, and 2.5 Å, respectively. All results correspond to the HF approximation using the 6-31G** basis set

2-RDM elements arising from this method as well as from the single and double excitation configuration interaction (CISD), single, double, and triple configuration interaction (CISDT), and FCI procedures, in order to compare their results with those of the GHV-EOM method; the comparison with experimental results would require the use of extended basis sets [39]. In systems possessing moderate correlations, like the H_n rings near the equilibrium geometry, it would be expected that after the incorporation of correlation effects the energies will not change significantly, i.e. the correlated bands should be very close to the HF ones. However, as we show, the inclusion of correlation effects is visible in the GHV-EOM bands. As dynamical Coulomb correlation is included, the effective mass of the electrons increases. In band theory, for simple parabolic bands, the effective mass tensor is defined as proportional to the inverse of the second derivative (Hessian matrix). Hence, the more mobile (lighter) electrons, the more dispersive bands (bigger bandwidths) and the more localized (heavier) electrons, the less dispersive bands (smaller bandwidths). To move a non-interacting electron turns out to be easier than to move an interacting one.

Electron-electron interaction, properly treated in GHV-EOM method, changes the band dispersion and corrects some shortcomings of the HF method. A well-known unphysical feature of the HF method is that, for extended systems in partially filled bands, HF density of states vanishes at the Fermi energy [44, 45], i.e. metallic systems in the HF method are gaped. In Fig. 3 (left), the 1S band of the H_{14} chain is plotted for different total number of electrons. For the neutral system, with the same number of electrons and atoms and net charge $C = 0$, it is easy to see a kink in the band dispersion around $ka = \pm\pi/2$. As the number of electrons increases the kink position moves towards the band edges, until the band is fully occupied. The kink occurs at a special k value, the so called “Fermi wave vector” k_F , which satisfies $\varepsilon(k_F) \equiv \varepsilon_F$, with ε_F the “Fermi energy”.

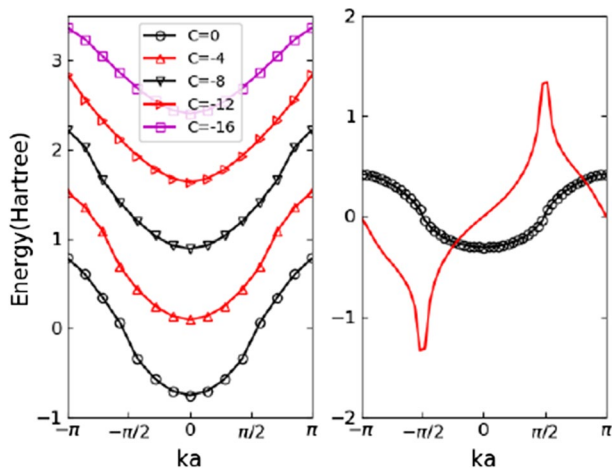


Fig. 3 Left: 1S band for the H₁₄ molecular ring with net charge C . Right: 1S band for the H₅₀ neutral system and its group velocity (in red), $v_k = \nabla_k \epsilon(k)$. Results correspond to the HF approximation at 1 Å between two neighbor atoms, using the 6-31G** and 6-31G basis sets for the H₁₄ and H₅₀ systems, respectively (Color figure online)

On the right side of Fig. 3, we have plotted the band dispersion of the neutral system H₅₀ (calculated with the 6-31G basis set) along with the group velocity $v_k = \nabla_k \epsilon(k)$. At k_F the velocity shows an instability, a logarithmic divergence, which in turns means the opening of a gap in the density of states at the Fermi energy. This unphysical feature is properly corrected including the correlation effects beyond HF.

Figure 4 shows results for the 1S band of H₁₄ ring obtained from different methods, using the STO-3G basis set (a single s-type atomic orbital assigned to each hydrogen atom). As correlations are included, even at the level of CISD and CISDT procedures, the unphysical kink in the band dispersion is smoothed out. For GHV-EOM results, this unphysical feature is completely removed and the band obtained is comparable to the FCI result. All this is more noticeable as the interatomic distance is increased, making correlations relatively more important. The incorporation of correlations in the band calculation introduces some general modifications on the band dispersion. As is already possible to see in Fig. 4 and more evidently in the 1S, 2S, and 2P bands of H₁₄ (see Fig. 5), correlated bands are less dispersive than uncorrelated ones. As discussed above, electrons are “heavier” when interactions are important. Moving an electron inside a solid involves not only its intrinsic inertia, its mass, but also the interactions with the surrounding particles. Even if electron-electron interactions are not considered, the simple interaction with the lattice makes the effective mass different from the intrinsic mass and the bands disperse. As electron correlations are incorporated, that effective mass may be enhanced, as can be seen in Fig. 5.

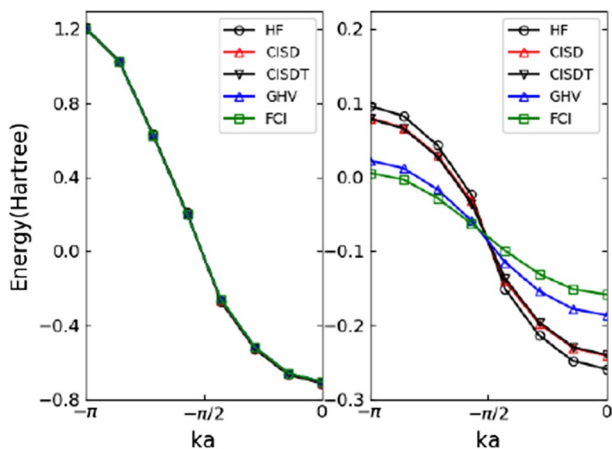


Fig. 4 1S band around the Fermi energy of the H_{14} ring molecule with net charge $C = 0$. Results correspond to the HF, CISD, CISDT, GHV, and FCI levels at 1 Å (left) and 2.5 Å (right) between two neighbor atoms, using the STO-3G basis set

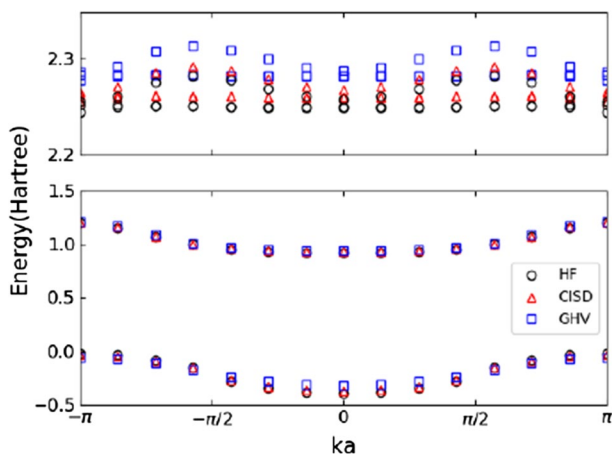


Fig. 5 1S, 2S, and 2P bands of the H_{14} ring molecule calculated with several methods. Results correspond to the HF, CISD, and GHV approximations at 2.5 Å between two neighbor atoms, using the 6-31G** basis set

5 Concluding remarks

This work incorporates the symmetry-adapted formulation for Abelian groups to the GHV-EOM treatment. The covariance of the resulting equations provides that all matrices involved in EOM method turn out to be invariant tensors possessing a block structure. This block factorization of the matrices associated with the reduced density matrices and electronic integrals used in this methodology leads to manage a considerably lower computational cost. The procedure has been successfully applied

to describe bands in cyclic chains of hydrogen atoms, which have been widely used as prototype models in condensed matter and other areas of interest. We perform an assessment of our proposal comparing our results with those arising from more conventional methods.

Acknowledgements This work has been financially supported by the Grant Nos. UBACYT 20020150100157BA, 20020190100214BA, and 20020170100284BA (Universidad de Buenos Aires, Argentina); Grants Nos. PIP 11220130100377CO, PIP 11220130100311CO, and 2013-1401PCB (Consejo Nacional de Investigaciones Científicas y Técnicas, Argentina); Grant Nos. PICT-201-0381 and PICT-2018-04536 (Agencia Nacional de Promoción Científica y Tecnológica, Argentina); Grant No. 1181165 (FONDECYT, Chile). E. R. and J. J. T. acknowledge support to Consejo Nacional de Investigaciones Científicas y Técnicas (Argentina) and Centro de Investigaciones Tecnológicas, Biomédicas y Medioambientales (Perú), respectively.

Compliance with ethical standards

Conflict of interest The authors have no conflicts of interest to declare that are relevant to the content of this article.









References

1. A.J. Coleman, *Rev. Mod. Phys.* **35**, 668 (1963)
2. E.R. Davidson, *Reduced Density Matrices in Quantum Chemistry* (Academic Press, New York, 1976)
3. A.J. Coleman, V.I. Yukalov, *Reduced Density Matrices: Coulson's Challenge* (Springer, New York, 2000)
4. *Many-electron Densities and Reduced Density Matrices*, ed. by J. Cioslowski (Kluwer, Dordrecht, The Netherlands, 2000)
5. *Advances in Chemical Physics*, ed. by D.A. Mazziotti, Vol. 134 (Wiley, New York, 2007)
6. C. Garrod, J.K. Percus, *J. Math. Phys.* **5**, 1756 (1964)
7. H. Nakatsuji, *Phys. Rev. A* **14**, 41 (1976)
8. J. Karwowski, W. Duch, C. Valdemoro, *Phys. Rev. A* **33**, 2254 (1986)
9. L. Lain, A. Torre, J. Karwowski, C. Valdemoro, *Phys. Rev. A* **38**, 2721 (1988)
10. H. Nakatsuji, K. Yasuda, *Phys. Rev. Lett.* **76**, 1039 (1996)
11. C. Valdemoro, L.M. Tel, E. Pérez-Romero, A. Torre, *J. Mol. Struct. (Theochem)* **537**, 1 (2001)
12. D.A. Mazziotti, *Chem. Rev.* **112**, 244 (2012)
13. D.R. Alcoba, C. Valdemoro, L.M. Tel, E. Pérez-Romero, *Int. J. Quantum Chem.* **109**, 3178 (2009)
14. D.A. Mazziotti, *Phys. Rev. Lett.* **97**, 143002 (2006)
15. C. Valdemoro, D.R. Alcoba, L.M. Tel, E. Pérez-Romero, *Int. J. Quantum Chem.* **109**, 2622 (2009)
16. D.R. Alcoba, L.M. Tel, E. Pérez-Romero, C. Valdemoro, *Int. J. Quantum Chem.* **111**, 937 (2011)
17. D.R. Alcoba, C. Valdemoro, L.M. Tel, E. Pérez-Romero, O.B. Oña, *J. Phys. Chem. A* **115**, 2599 (2011)
18. C. Valdemoro, D.R. Alcoba, O.B. Oña, L.M. Tel, E. Pérez-Romero, J.M. Oliva, *Chem. Phys.* **399**, 59 (2012)
19. J. Simons, W.D. Smith, *J. Chem. Phys.* **58**, 4899 (1973)
20. C. Valdemoro, D.R. Alcoba, L.M. Tel, *Int. J. Quantum Chem.* **112**, 2965 (2012)
21. G.E. Massaccesi, D.R. Alcoba, O.B. Oña, *J. Math. Chem.* **50**, 2155 (2012)
22. D.R. Alcoba, G.E. Massaccesi, O.B. Oña, J.J. Torres-Vega, L. Lain, A. Torre, *J. Math. Chem.* **52**, 1794 (2014)
23. A.V. Sinititskiy, L. Greenman, D.A. Mazziotti, *J. Chem. Phys.* **133**, 014104 (2010)
24. M. Motta, D.M. Ceperley, G. Kin-Lic Chan, J.A. Gomez, E. Gull, S. Guo, C.A. Jiménez-Hoyos, T.N. Lan, J. Li, F. Ma, A.J. Millis, N.V. Prokof'ev, U. Ray, G.E. Scuseria, S. Sorella, E.M. Stoudenmire, Q. Sun, I.S. Tupitsyn, S.R. White, D. Zgid, S. Zhang, *Phys. Rev. X* **7**, 031059 (2017)

25. R. Quintero-Monsebaiz, I. Mitzelena, M. Rodríguez-Mayorga, A. Vela, M. Piris, J. Phys.: Condens. Matter **31**, 165501 (2019)
26. I. Mitzelena, M. Piris, J. Phys.: Condens. Matter **32**, 17LT01 (2020)
27. M. Motta, C. Genovese, F. Ma, Z.H. Cui, R. Sawaya, G. Kin-Lic Chan, N. Chepiga, P. Helms, C. Jiménez-Hoyos, A.J. Millis, U. Ray, E. Ronca, H. Shi, S. Sorella, E.M. Stoudenmire, S.R. White, S. Zhang, Phys. Rev. X **10**, 031058 (2020)
28. P.R. Surjan, *Second Quantized Approach to Quantum Chemistry: An Elementary Introduction* (Springer, Berlin, 1989)
29. M.V. Mihailovic, M. Rosina, Nucl. Phys. A **130**, 386 (1969)
30. D.R. Alcoba, C. Valdemoro, Phys. Rev. A **64**, 062105 (2001)
31. F. Colmenero, C. Pérez del Valle, C. Valdemoro, Phys. Rev. A **47**, 971 (1993)
32. D.A. Mazziotti, Phys. Rev. A **60**, 3618 (1999)
33. C. Valdemoro, L. M. Tel, E. Pérez-Romero, in *Many-electron Densities and Density Matrices*, ed. by J. Cioslowski (Kluwer, Boston, 2000)
34. D.J. Rowe, Rev. Mod. Phys. **40**, 153 (1968)
35. D.J. Rowe, *Nuclear Collective Motion Models and Theory* (Methuen and Co., London, 1970)
36. Z. Szekeres, A. Szabados, M. Kállay, P.R. Surjan, Phys. Chem. Chem. Phys. **3**, 696 (2001)
37. J. Simons, Adv. Quantum Chem. **50**, 213 (2005)
38. D.A. Mazziotti, Phys. Rev. A **68**, 052501 (2003)
39. J.D. Farnum, D.A. Mazziotti, Chem. Phys. Lett. **400**, 90 (2004)
40. S. Hemmatiyani, M. Sajjan, A.W. Schlimgen, D.A. Mazziotti, J. Phys. Chem. Lett. **9**, 5373 (2018)
41. L.M. Tel, E. Pérez-Romero, F.J. Casquero, C. Valdemoro, Phys. Rev. A **67**, 052504 (2003)
42. M. Springborg, *Methods of Electronic-Structure Calculations: From Molecules to Solids* (Wiley, New York, 2000)
43. N.W. Ashcroft, N.D. Mermin, *Solid State Physics* (Harcourt College Publishers, Florida, 1976)
44. H.J. Monkhorst, Phys. Rev. B **20**, 1504 (1979)
45. V. Bezugly, U. Birkenheuer, Chem. Phys. Lett. **399**, 57 (2004)

Publisher's Note Springer Nature remains neutral with regard to jurisdictional claims in published maps and institutional affiliations.

Affiliations

Juan J. Torres-Vega¹  · Gustavo E. Massaccesi²  · Elías Ríos³  ·
Alberto Camjayi^{4,5}  · Alicia Torre⁶  · Luis Lain⁶  · Ofelia B. Oña³  ·
William Tiznado⁷  · Diego R. Alcoba^{4,5} 

¹ Centro de Investigaciones Tecnológicas, Biomédicas y Medioambientales, c/ José Santos Chocano 199, Callao, Peru

² Departamento de Ciencias Exactas, Ciclo Básico Común, Universidad de Buenos Aires, Ciudad Universitaria, 1428 Buenos Aires, Argentina

³ Instituto de Investigaciones Fisicoquímicas Teóricas y Aplicadas, Universidad Nacional de La Plata, Consejo Nacional de Investigaciones Científicas y Técnicas, Diag. 113 y 64 (S/N), Sucursal 4, CC 16, 1900 La Plata, Argentina

⁴ Departamento de Física, Facultad de Ciencias Exactas y Naturales, Universidad de Buenos Aires, Ciudad Universitaria, 1428 Buenos Aires, Argentina

⁵ Instituto de Física de Buenos Aires, Consejo Nacional de Investigaciones Científicas y Técnicas, Ciudad Universitaria, 1428 Buenos Aires, Argentina

⁶ Departamento de Química Física, Facultad de Ciencia y Tecnología, Universidad del País Vasco, Apdo. 644, 48080 Bilbao, Spain

- ⁷ Departamento de Química, Facultad de Ciencias Exactas, Universidad Andres Bello, Avda. República 498, Santiago, Chile